Table 3
Numbers and areas of GST-P positive foci in the livers of F344 rats treated with APNH [26]

Treatment	No. of rats	GST-P-positive foci	
		Number/cm^2	mm^2/cm^2
Control diet	3	0	0
10 ppm APNH	5	0.52 ± 0.03	0.006 ± 0.01
20 ppm APNH	5	1.3 ± 0.9	0.01 ± 0.01
50 ppm APNH	6	21 ± 5.8	2.3 ± 1.3

Values are mean ± S.D. for foci larger than 0.1 mm in diameter.

and serum follicle-stimulating hormone and luteinizing hormone levels were not affected, so that disruption of spermatogenesis might not be related to hypothalamic-pituitary dysfunction. The morphological alterations in rats given APNH were similar to those caused by Sertoli cell toxicants, such as 1,3-dinitrobenzene and 2,5-hexanedione. In addition, erosive changes in urinary bladder, thymic atrophy, and panmyelophthisis were observed.

When 7-week-old male rats were fed diets containing 10 ppm, 20 ppm or 50 ppm of APNH for 4 weeks, clear cell or mixed type foci were observed in the livers. Almost all of these foci stained immunohistochemically positive for glutathione S-transferase placental (GST-P) form [26]. In livers of rats fed the control diet, no such GST-P-positive altered foci larger than 0.1 mm in diameter were found. The data for induction of liver GST-P-positive foci in rats by APNH are summarized in Table 3. In organs other than the liver, there is no evidence of toxicity or carcinogenicity in this medium-term assay. MeIQx, one mutagenic and carcinogenic HA, at a dietary dose of 400 ppm long-term induced liver tumors in 100% in male F344 rats [27]. GST-P-positive foci were first observed after 12 weeks, whereas APNH at doses of 10–50 ppm for 4 weeks clearly produced GST-P-positive foci in the liver in a dose-dependent manner, with quantitative values for the dose of 50 ppm after 4 weeks comparable to those with 400 ppm MeIQx for 12 weeks [28]. Moreover, 40 ppm of MeIQx did not induce GST-P-positive foci in the liver of rats [29]. This comparison indicates that APNH might be a much more potent liver carcinogen than other HAs, such as MeIQx. Indeed, APNH was recently demonstrated to induce liver tumors in F344 rats when given at doses of 20 and 40 ppm in diet for 85 weeks (our unpublished data).

7. Discussion

We summarized here that in this survey the mutagenicity of β-carbolines with aromatic amines in the presence of S9 mix is due to the formation of novel mutagenic aminophenyl-β-carboline derivatives. In addition, APNH, the most potent of the coupled compounds formed from β-carboline and aromatic amines, demonstrated severe tox-

icity in testes and carcinogenicity in the livers of F344 rats. The in vivo toxicity of APNH was much higher than that of other mutagenic HAs, such as MeIQx. It has been reported that norharman also shows co-mutagenicity with 3-aminopyridine, 2-amino-3-methylpyridine, yellow OB and N,N-diphenylamine, in the presence of S9 mix [1,3]. Although the mechanisms underlying the appearance of mutagenicity by these reactions remain to be clarified, it is likely that similar derivatives to APNH could be formed in presence of S9 mix.

As mentioned above, both β-carbolines and aromatic amines are widely present in food and cigarette smoke and therefore it is likely that humans are simultaneously exposed to both, so that aminophenyl-β-carboline derivatives may be produced in our bodies. N-Nitroso compounds are well known as endogenous mutagens and carcinogens, and aminophenyl-β-carboline derivatives may be classified for one of the novel type of endogenous mutagens and carcinogens. Based on the yields of APNH, exposure levels may be lower than with HAs but their health risk in terms of human cancer development might be comparable, because of the stronger genotoxic activity of APNH than HAs. To clarify the effects of APNH and its derivatives on human health, it is important to further elucidate their detailed biological properties.

References

[1] M. Nagao, T. Yahagi, T. Sugimura, Biochem. Biophys. Res. Comm. 83 (1978) 373.
[2] M. Nagao, T. Yahagi, M. Honda, Y. Seino, T. Matsushima, T. Sugimura, Proc. Jpn. Acad. 53B (1997) 34.
[3] T. Sugimura, M. Nagao, K. Wakabayashi, in: R. Snyder, D.J. Jollow, D.V. Parke, C.G. Gibson, J.J. Kocsis, C.M. Witmer (Eds.), Biological Reactive Intermediates-II, Chemical Mechanisms and Biological Effects (Part B). Plenum Press, NY, 1982, p. 1011.
[4] Y. Totsuka, H. Ushiyama, J. Ishihara, R. Sinha, S. Goto, T. Sugimura, K. Wakabayashi, Cancer Lett. 143 (1999) 139.
[5] H. Ushiyama, A. Oguri, Y. Totsuka, H. Itoh, T. Sugimura, K. Wakabayashi, Proc. Jpn. Acad. 71B (1995) 57.
[6] W. Pfau, K. Skog, J. Chromatogr. B (2003) in press.
[7] F. Luceri, P. Giuseppe, G. Moneti, P. Dolara, Toxicol. Ind. Health 9 (1993) 405.
[8] IARC (International Agency for Research on Cancer), IARC Monographs on the Evaluation of Carcinogenic Risks of Chemicals to Humans, vol. 27, IARC, Lyon, 1982, p. 39.
[9] IARC Monographs on the Evaluation of Carcinogenic Risks of Chemicals to Humans, vol. 27, IARC, Lyon, 1982, p. 155.
[10] M. Riffelmann, G. Muller, W. Schmieding, W. Popp, K. Norpoth, Int. Arch. Occup. Environ. Health 68 (1995) 36.
[11] K.E. Bayoumy, J.M. Donahue, S.S. Hecht, D. Hoffmann, Cancer Res. 46 (1986) 6064.

[12] L.S. DeBruin, J.B. Pawliszyn, P.D. Josephy, Chem. Res. Toxicol. 12 (1999) 78.

[13] R. Kato, Y. Yamazoe, Jpn. J. Cancer Res. (Gann) 78 (1987) 297.

[14] Y. Totsuka, N. Hada, K. Matsumoto, N. Kawahara, Y. Murakami, Y. Yokoyama, T. Sugimura, K. Wakabayashi, Carcinogenesis 19 (1998) 1995.

[15] T. Sugimura, Environ. Health Perspect. 106 (1998) A522.

[16] N. Hada, Y. Totsuka, T. Enya, K. Tsurumaki, M. Nakazawa, Mutat. Res. 493 (2001) 115.

[17] K. Wakabayashi, M. Nagao, H. Esumi, T. Sugimura, Cancer Res. 52 (1992) 2092s.

[18] M. Mori, Y. Totsuka, K. Fukutome, T. Yoshida, T. Sugimura, K. Wakabayashi, Carcinogenesis 17 (1996) 1499.

[19] Y. Totsuka, T. Takamura-Enya, N. Kawahara, R. Nishigaki, T. Sugimura, K. Wakabayashi, Chem. Res. Toxicol. 15 (2002) 1288.

[20] T. Ohe, T. Takata, Y. Maeda, Y. Totsuka, N. Hada, A. Matsuoka, N. Tanaka, K. Wakabayashi, Mutat. Res. 515 (2002) 181.

[21] Y. Totsuka, T. Kataoka, T. Enya-Takamura, T. Sugimura, K. Wakabayashi, Mutat. Res. 506-507 (2002) 49.

[22] F.P. Guengerich, Chem. Res. Toxicol. 14 (2001) 611.

[23] T. Aoyama, F.J. Gonzalez, H.V. Gelboin, Mol. Carcinog. 1 (1989) 253.

[24] Y. Oda, Y. Totsuka, K. Wakabayashi, T. Shimada, Mutat. Res. 483 (Suppl.1) (2001) S132.

[25] Y. Totsuka, T. Kawamori, S. Hisada, K. Mitsumori, J. Ishihara, T. Sugimura, K. Wakabayashi, Toxicol. Appl. Pharmacol. 175 (2001) 169.

[26] T. Kawamori, Y. Totsuka, J. Ishihara, N. Uchiya, T. Sugimura, K. Wakabayashi, Cancer Lett. 163 (2000) 157.

[27] H. Ohgaki, S. Takayama, T. Sugimura, Mutat. Res. 259 (1991) 399.

[28] M. Hirose, K. Wakabayashi, M. Ochiai, H. Kushida, T. Sato, T. Sugimura, M. Nagao, Jpn. J. Cancer Res. 86 (1995) 516.

[29] H. Sone, K. Wakabayashi, H. Kushida, T. Sugimura, M. Nagao, Carcinogenesis 13 (1992) 793.

Differential contributions of Mesp1 and Mesp2 to the epithelialization and rostro-caudal patterning of somites

Yu Takahashi[1,*], Satoshi Kitajima[1], Tohru Inoue[1], Jun Kanno[1] and Yumiko Saga[2,*]

[1]Cellular & Molecular Toxicology Division, National Institute of Health Sciences, 1-18-1 Kamiyoga, Setagayaku, Tokyo 158-8501, Japan
[2]Division of Mammalian Development, National Institute of Genetics, Yata 1111, Mishima 411-8540, Japan
*Authors for correspondence (e-mail: yutak@nihs.go.jp and ysaga@lab.nig.ac.jp)

Summary

Mesp1 and Mesp2 are homologous basic helix-loop-helix (bHLH) transcription factors that are co-expressed in the anterior presomitic mesoderm (PSM) just prior to somite formation. Analysis of possible functional redundancy of Mesp1 and Mesp2 has been prevented by the early developmental arrest of Mesp1/Mesp2 double–null embryos. Here we performed chimera analysis, using either Mesp2-null cells or Mesp1/Mesp2 double–null cells, to clarify (1) possible functional redundancy and the relative contributions of both Mesp1 and Mesp2 to somitogenesis and (2) the level of cell autonomy of Mesp functions for several aspects of somitogenesis. Both Mesp2-null and Mesp1/Mesp2 double–null cells failed to form initial segment borders or to acquire rostral properties, confirming that the contribution of Mesp1 is minor during these events. By contrast, Mesp1/Mesp2 double–null cells contributed to neither epithelial somite nor dermomyotome formation, whereas Mesp2-null cells partially contributed to incomplete somites and the dermomyotome. This indicates that Mesp1 has a significant role in the epithelialization of somitic mesoderm. We found that the roles of the Mesp genes in epithelialization and in the establishment of rostral properties are cell autonomous. However, we also show that epithelial somite formation, with normal rostro-caudal patterning, by wild-type cells was severely disrupted by the presence of Mesp mutant cells, demonstrating non-cell autonomous effects and supporting our previous hypothesis that Mesp2 is responsible for the rostro-caudal patterning process itself in the anterior PSM, via cellular interaction.

Key words: Somitogenesis, Epithelial-mesenchymal conversion, Mesp2, Chimera analysis, Mouse

Introduction

Somitogenesis is not only an attractive example of metameric pattern formation but is also a good model system for the study of morphogenesis, particularly epithelial-mesenchymal interconversion in vertebrate embryos (Gossler and Hrabe de Angelis, 1997; Pourquié, 2001). The primitive streak, or tailbud mesenchyme, supplies the unsegmented paraxial mesoderm, known as presomitic mesoderm (PSM). Mesenchymal cells in the PSM undergo mesenchymal-epithelial conversion to form epithelial somites in a spatially and temporally coordinated manner. Somites then differentiate, in accordance with environmental cues from the surrounding tissues, into dorsal epithelial dermomyotome and ventral mesenchymal sclerotome (Borycki and Emerson, 2000; Fan and Tessier Lavigne, 1994). Hence, the series of events that occur during somitogenesis provide a valuable example of epithelial-mesenchymal conversion. The dermomyotome gives rise to both dermis and skeletal muscle, whereas the sclerotome forms cartilage and bone in both the vertebrae and the ribs. Each somite is subdivided into two compartments, the rostral (anterior) and caudal (posterior) halves. This rostro-caudal polarity appears to be established just prior to somite formation (Saga and Takeda, 2001).

Mesp1 and Mesp2 are closely related members of the basic helix-loop-helix (bHLH) family of transcription factors but share significant sequence homology only in their bHLH regions (Saga et al., 1996; Saga et al., 1997). During development of the mouse embryo, both Mesp1 and Mesp2 are specifically expressed in the early mesoderm just after gastrulation and in the paraxial mesoderm during somitogenesis. Mesp1/Mesp2 double-null embryos show defects in early mesodermal migration and thus fail to form most of the embryonic mesoderm, leading to developmental arrest (Kitajima et al., 2000). Mesp1-null embryos exhibit defects in single heart tube formation, due to a delay in mesodermal migration, but survive to the somitogenesis stage (Saga et al., 1999), suggesting that there is some functional redundancy, i.e. compensatory functions of Mesp2 in early mesoderm. During somitogenesis, both Mesp1 and Mesp2 are expressed in the anterior PSM just prior to somite formation. Although we have shown that Mesp2, but not Mesp1, is essential for somite formation and the rostro-caudal patterning of somites (Saga et al., 1997), a possible functional redundancy between Mesp1 and Mesp2 has not yet been clearly established.

To further clarify the contributions of Mesp1 and Mesp2 to somitogenesis, analysis of Mesp1/Mesp2 double-null embryos

is necessary, but because of the early mesodermal defects already described, these knockout embryos lack a paraxial mesoderm, which prevents any analysis of somitogenesis. We therefore adopted a strategy that utilized chimera analysis. As we have reported previously, the early embryonic lethality of a Mesp1/Mesp2 double knockout is rescued by the presence of wild-type cells in a chimeric embryo, but the double-null cells cannot contribute to the cardiac mesoderm (Kitajima et al., 2000). This analysis, however, focused only on early heart morphogenesis and did not investigate the behavior of Mesp1/Mesp2 double-null cells in somitogenesis. In this report, we focus upon somitogenesis and compare two types of chimeras using either Mesp1/Mesp2 double-null cells or Mesp2-null cells to investigate Mesp1 function during somitogenesis.

Another purpose of our chimera experiments was to elucidate the cell autonomy of Mesp functions. In the process of somite formation, mesenchymal cells in the PSM initially undergo epithelialization at the future segment boundary, independently of the already epithelialized dorsal or ventral margin of the PSM (Sato et al., 2002). Epithelial somite formation is disrupted in the Mesp2-null embryo, indicating that Mesp2 is required for epithelialization at the segment boundary. Although Mesp products are nuclear transcription factors and their primary functions must therefore be cell autonomous (transcriptional control of target genes), it is possible that the roles of Mesp2 in epithelialization are mediated by the non-cell autonomous effects of target genes. We therefore asked whether the defects in Mesp2-null cells during epithelialization could be rescued by the presence of surrounding wild-type cells. Additionally, we would expect to find that the role of Mesp2 in establishing rostro-caudal polarity is rescued in a similar way.

Our analysis suggests that Mesp1 and Mesp2 have redundant functions and are both cell-autonomously involved in the epithelialization of somitic mesoderm. In addition, our results highlight some non-cell autonomous effect of Mesp2-null and Mesp1/Mesp2-null cells.

Materials and methods

Generation of chimeric embryos

As described previously (Kitajima et al., 2000), chimeric embryos were generated by aggregating 8-cell embryos of wild-type mice (ICR) with those of mutant mice that were genetically marked with the ROSA26 transgene (Zambrowicz et al., 1997). Mesp1/Mesp2 double-null embryos were generated by crossing wko-del (+/−) and Mesp1(+/−)/Mesp2(+/cre) mice as described previously (Kitajima et al., 2000). This strategy enables us to distinguish chimeric embryos derived from homozygous embryos, which have two different mutant alleles, from those derived from heterozygous embryos. Likewise, Mesp2-null embryos were generated by crossing P2vl(+/−) mice (Saga et al., 1997) and P2GFP (+/gfp) mice (Y.S. and S.K., unpublished) that were also labeled with the ROSA26 locus. The genotype of the chimeric embryos was determined by PCR using yolk sac DNA.

Histology, histochemistry and gene expression analysis

The chimeric embryos were fixed at 11 days postcoitum (dpc) and stained in X-gal solution for the detection of β-galactosidase activity, as described previously (Saga et al., 1999). For histology, samples stained by X-gal were postfixed with 4% paraformaldehyde, dehydrated in an ethanol series, embedded in plastic resin (Technovit

8100, Heraeus Kulzer) and sectioned at 3 μm. The methods used for gene expression analysis by in-situ hybridization of whole-mount samples and frozen sections and skeletal preparation by Alcian Blue/Alizarin Red staining were described previously (Saga et al., 1997; Takahashi et al., 2000). Probes for in-situ hybridization for Uncx4.1 (Mansouri et al., 1997; Neidhardt et al., 1997), Delta-like 1 (Dll1) (Bettenhausen et al., 1995) and Paraxis (Burgess et al., 1995) were kindly provided by Drs Peter Gruss, Achim Gossler and Alan Rawls, respectively. A probe for EphA4 (Nieto et al., 1992) was cloned by PCR. For detection of actin filaments, frozen sections were stained with AlexaFluor 488-conjugated phalloidin (Molecular Probes) according to the manufacturer's protocol.

Results

Possible functional redundancy and different contributions of Mesp1 and Mesp2 in somitogenesis

During somitogenesis, both Mesp1 and Mesp2 are expressed in the anterior PSM just prior to somite formation and their expression domains overlap (Fig. 1A). Mesp1-null embryos form morphologically normal somites and show normal rostro-caudal patterning within each somite (Fig. 1B,E-H), indicating that Mesp1 is not essential for somitogenesis. By contrast, Mesp2 is essential for both the formation and rostro-caudal patterning of somites, as Mesp2-null embryos have no epithelial somites and lose rostral half properties, resulting in caudalization of the entire somitic mesoderm (Saga et al., 1997) (Fig. 1C,D).

Although somite formation and rostro-caudal patterning is disrupted in the Mesp2-null embryo, histological differentiation into dermomyotome and sclerotome is not affected. It is noteworthy that the Mesp2-null embryo still forms disorganized dermomyotomes without forming epithelial somites (Saga et al., 1997). As Mesp1 is expressed at normal levels in the PSM of Mesp2-null embryos (Fig. 1C,D), it is possible that Mesp1 functions to rescue some aspects of somitogenesis in the Mesp2-null embryo. In order to further clarify the contributions of both Mesp1 and Mesp2 during somitogenesis, we therefore generated chimeric embryos with either Mesp2-null cells or Mesp1/Mesp2 double-null cells and compared the behavior of mutant cells during somitogenesis (Fig. 2).

Mesp2-null cells tend to be eliminated from the epithelial somite and the dermomyotome, but can partially contribute to both of these structures

We first generated Mesp2-null chimeric embryos ($Mesp2^{-/-}$ with Rosa26: wild) to analyze cell autonomy of Mesp2 function during somitogenesis. The control chimeric embryo ($Mesp2^{+/-}$ with Rosa26: wild) showed normal somitogenesis and a random distribution of X-gal stained cells (Fig. 3A). The Mesp2-null chimeric embryos formed abnormal somites that exhibited incomplete segmentation (Fig. 3B), but histological differentiation of dermomyotome and sclerotome was observed. Within the incomplete somite, X-gal-stained Mesp2-null cells were mainly localized in the rostral and central regions, surrounded by wild-type cells at the dorsal, ventral and caudal sides (Fig. 3B). The surrounding wild-type cells, however, did not form an integrated epithelial sheet, but consisted of several epithelial cell clusters. Such trends were more obviously observed in other sections, where wild-type cells were found to form multiple small epithelial clusters (Fig.
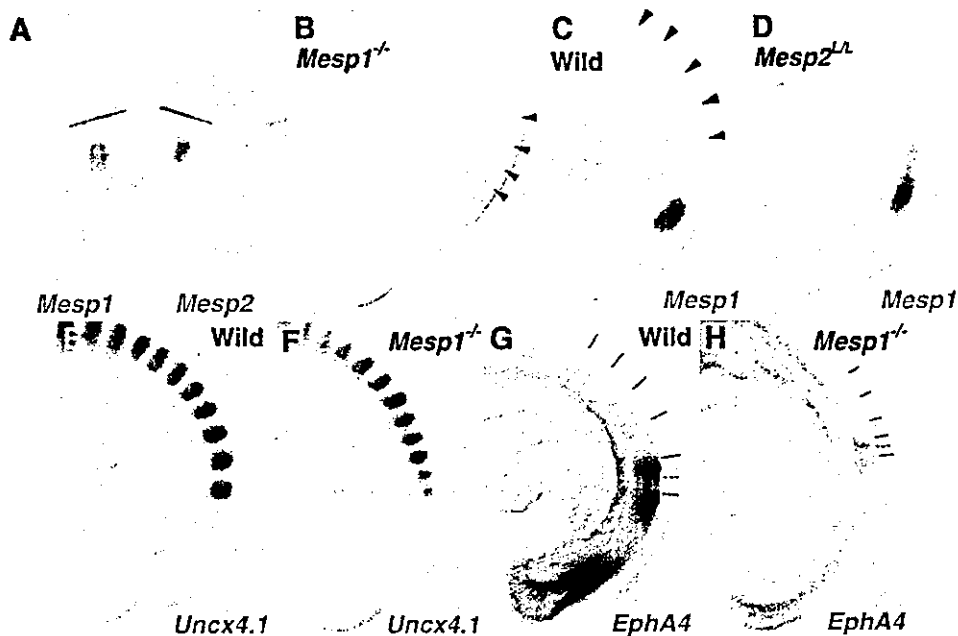
Fig. 1. *Mesp1* and *Mesp2* are co-expressed in the anterior PSM but have differing roles in somitogenesis. (A) Overlapping expression of *Mesp1* and *Mesp2* is revealed by in-situ hybridization using the left and right halves of the same embryo. The lines show most recently formed somite boundaries. (B-C) A Mesp1-null embryo (B) shows the same normal somite formation as a wild-type embryo (C). Arrowheads indicate somite boundaries. (D) In Mesp2-null embryos, no somite formation is observed but *Mesp1* is expressed at comparable levels to wild type, although its expression is anteriorly extended and blurred. (E-H) Mesp1-null embryos show normal rostro-caudal patterning of somites. (E,F) Expression of a caudal half marker, *Uncx4.1*. (G,H) Expression of a rostral half marker, *EphA4*. The lines indicate presumptive or formed somite boundaries and the dotted line indicates approximate position of somite half boundary.

3C,D). Mesp2-null cells tended to be eliminated from the epithelial clusters, although they were partially integrated into these structures (blue arrows in Fig. 3C,D). Likewise, small numbers of Mesp2-null cells were found to contribute to the dermomyotome (Fig. 3E,F). Mesp2-null cells also appeared to form the major part of the sclerotome.

Mesp2 is required for the cell-autonomous acquisition of rostral properties

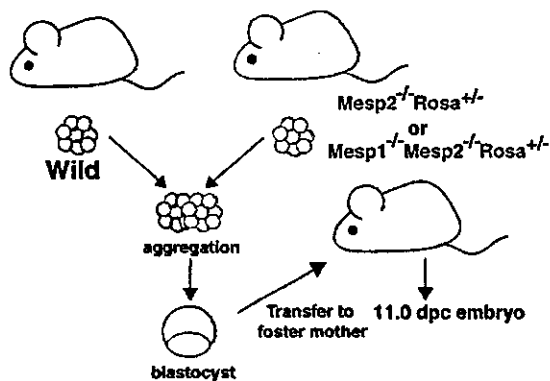We have previously demonstrated that suppression by Mesp2

Fig. 2. Schematic representation of chimera analysis method. Either Mesp2-null or Mesp1/Mesp2 double-null embryos, genetically labeled with *Rosa* locus, were aggregated with wild-type embryos at the 8-cell stage, and the resulting chimeras were subjected to analysis at 11.0 dpc.

of the caudal genes *Dll1* and *Uncx4.1* in presumptive rostral half somites is a crucial event in the establishment of the rostro-caudal pattern of somites (Saga et al., 1997; Takahashi et al., 2000). As Mesp2-null embryos exhibit caudalization of somites, Mesp2-null cells are predicted to be unable to express rostral properties. Hence, Mesp2-null cells are expected to distribute to the caudal region of each somite where the rostro-caudal patterns are rescued by wild-type cells in a chimeric embryo. In this context, the localization of Mesp2-null cells at the rostral side was an unexpected finding. We interpret this to mean that the rostral location of Mesp2-null cells is due to a lack of epithelialization functions (see Discussion).

To examine rostro-caudal properties in Mesp2-null cells, located in the rostral side, we analyzed the expression of a caudal half marker gene, *Uncx4.1* (Mansouri et al., 1997; Neidhardt et al., 1997). Analysis of adjacent sections revealed that *lacZ*-expressing Mesp2-null cells, localized at the rostral and central portion, ectopically expressed *Uncx4.1* (Fig. 4A-D). This strongly suggests that Mesp2-null cells cannot acquire rostral properties even if surrounded by wild-type cells, and that Mesp2 function is cell-autonomously required for the acquisition of rostral properties. We also observed that the small number of Mesp2-null cells distributed mostly to the caudal end of the dermomyotome (Fig. 3E,F) and that the expression pattern of *Uncx4.1* was normal in the dermomyotome (Fig. 4E,F). In the sclerotome, *lacZ*-expressing Mesp2-null cells often distributed to the rostral side, where expression of *Uncx4.1* was abnormally elevated (Fig. 4G,H). The vertebrae of the Mesp2-null chimeric fetus showed a partial fusion of the neural arches, which was reminiscent of

Mesp2-hypomorphic fetuses (Fig. 4I,J) (Nomura-Kitabayashi et al., 2002). Fusion of proximal rib elements was also observed (Fig. 4K,L).

Mesp1/Mesp2 double-null cells cannot contribute to the formation of epithelial somites or to the dermomyotome

To address the question of whether Mesp1, in addition to Mesp2, exhibits any function during somitogenesis, we next generated Mesp1/Mesp2 double-null chimeric embryos and compared them with the Mesp2-null chimeric embryos described in the previous sections. We first performed whole-mount X-gal staining of embryos at 11 dpc. In the control chimeric embryo, the X-gal-stained Mesp1/Mesp2 double-heterozygous cells distributed randomly throughout the embryonic body, including the somite region (Fig. 5A,C). By contrast, the Mesp1/Mesp2

double-null chimeric embryo displayed a strikingly uneven pattern of cellular distribution in the somite region. The X-gal stained Mesp1/Mesp2 double-null cells were localized at the medial part of embryonic tail and were not observed in the lateral part of the somite region (Fig. 5B,D). Histological examination of parasagittal sections further revealed obvious differences in the cellular contribution to somite formation (Fig. 5E,F). In the control chimeric embryo, Mesp1/Mesp2 double-heterozygous cells distributed randomly throughout the different stages of somitogenesis (PSM, somite, dermomyotome and sclerotome: Fig. 5E). In the Mesp1/Mesp2 double-null chimeric embryo, neither the initial segment border nor epithelial somites were formed, but histologically distinguishable dermomyotome-like and sclerotome-like compartments were generated (Fig. 5F). In addition, Mesp1/Mesp2 double-null cells and wild-type cells were randomly mixed in the PSM, whereas the dermomyotome-like epithelium consisted exclusively of wild-type cells and the sclerotome-like compartment consisted mostly of Mesp1/Mesp2 double-null cells. This suggests that either Mesp1 or Mesp2 is cell-autonomously required for the formation of epithelial somite and dermomyotome. These results also indicate that PSM cells with different characteristics are rapidly sorted during somite formation.

Subsequent examination of transverse sections confirmed the elimination of Mesp1/Mesp2 double-null cells from dermomyotome (Fig. 5G,H). In the mature somite region, the wild-type dermomyotome-like epithelium was found to form the myotome (my) (Fig. 5I,J). Furthermore, the ventral part of this dermomyotome-like epithelium became mesenchymal and appeared to contribute to the dorsal sclerotome (dsc), implying that this initial dermomyotome-like epithelium actually corresponds to the epithelial somite exclusively composed of wild-type cells (Fig. 5I,J). Fluorescent phalloidin staining revealed that the apical localization of actin filaments is limited to the dorsal compartments, which are occupied by wild-type cells in the Mesp1/Mesp2 double-null chimeric embryo (Fig. 5K,L), indicating the Mesp1/Mesp2 double-null cells cannot undergo epithelialization.

It is known that the bHLH transcription factor paraxis (Tcf15 – Mouse Genome Informatics), is required for the epithelialization of somite and

Mesp2$^{+/-}$: Wild

A

B **Mesp2$^{-/-}$: Wild**

C **D**

E **F**

Fig. 3. Mesp2-null cells tend to be excluded from the epithelial region of the somites. (A) The control chimeric embryo undergoes normal somite formation and shows random distribution of labeled cells. The right panel is a high-power view of a somite. (B) In the Mesp2-null chimeric embryo, incompletely segmented somites are formed. Mesp2-null cells tend to be localized at the rostral and central region of these incomplete segments. Red arrows: wild-type cell clusters; blue arrows: Mesp2-null cell clusters. (C,D) Other sections indicating multiple small epithelial cell clusters (arrows). Note that Mesp2-null cells only partially contribute to the epithelial clusters (blue arrows). (E,F) A small number of Mesp2-null cells are distributed in the dermomyotome and are mostly localized at the caudal end. Scale bars: 100 μm.

dermomyotome (Burgess et al., 1995; Burgess et al., 1996). Although *Paraxis* expression is not affected in Mesp2-null embryos (data not shown), it is possible that it is influenced by the loss of both Mesp1 and Mesp2. We therefore examined the expression patterns of *Paraxis* in our Mesp1/Mesp2 double-null chimeras. In wild-type embryos *Paraxis* is initially expressed throughout the entire somite region (in both the prospective dermomyotomal and sclerotomal regions) in the anteriormost PSM and newly forming somites, and then localizes in the dermomyotomes (Burgess et al., 1995). The dorsal dermomyotomal epithelium, composed of wild–type cells, strongly expressed *Paraxis* in the chimeric embryo (Fig. 6A,B). In addition, adjacent sections revealed that *lacZ*-expressing Mesp1/Mesp2 double-null cells expressed *Paraxis* in the medial sclerotomal compartment (Fig. 6A,B, brackets). This suggests that *Paraxis* expression in the future sclerotomal region is independent of Mesp factors. However, at present we cannot exclude the possibility that the maintenance of *Paraxis* expression in the dermomyotome requires the functions of either Mesp1 or Mesp2.

Mesp1/Mesp2 double-null cells are incapable of acquiring rostral properties

To clarify the rostro-caudal properties of somites in our chimeric embryos, we examined the expression pattern of *Uncx4.1*. Control chimeric embryos exhibited a normal stripe pattern of *Uncx4.1* expression throughout the segmented somite region (Fig. 7A). By contrast, Mesp1/Mesp2 double-null chimeric embryos exhibited continuous *Uncx4.1* expression in the ventral sclerotomal region (Fig. 7B). This continuity was observed in the entire sclerotome-like compartment of the newly formed somite region and in the ventral sclerotome in the mature somite region. The caudal localization of *Uncx4.1* expression, however, was normal in the dermomyotome and the dorsal sclerotome, which consisted of wild-type cells (Fig. 5), even in Mesp1/Mesp2 double-null chimeras. This suggests that, like Mesp2-null cells, Mesp1/Mesp2 double-null cells are incapable of acquiring rostral properties. Since the mesoderm of Mesp1/Mesp2 double-null embryos lacks the expression of the major markers of paraxial mesoderm (Kitajima et al., 2000), and Mesp1/Mesp2 double-null cells do not exhibit histological features characteristic of epithelial somites in our current study, it is possible that Mesp1/Mesp2 double-null cells may lack

paraxial mesoderm properties. However, the analysis of adjacent sections suggests that *lacZ*-expressing Mesp1/Mesp2 double-null cells themselves express *Uncx4.1*, a somite-specific marker (Fig. 7C,D), and they had also been found to have normal expression of *Paraxis* (Fig. 6A,B).

It is believed that the rostro-caudal pattern within somites and dermomyotomes is generated in the PSM and maintained in somites and dermomyotomes. We observed a normal rostro-caudal pattern in the dermomyotome (Fig. 7), although wild-type cells and Mesp1/Mesp2 double-null cells are mixed in the PSM (Fig. 5), of Mesp1/Mesp2 double-null chimeric embryos. As Mesp products are required for suppression of *Dll1* in the anterior PSM, a normal Dll1 stripe pattern cannot be formed if Mesp1/Mesp2 double-null cells are randomly distributed in

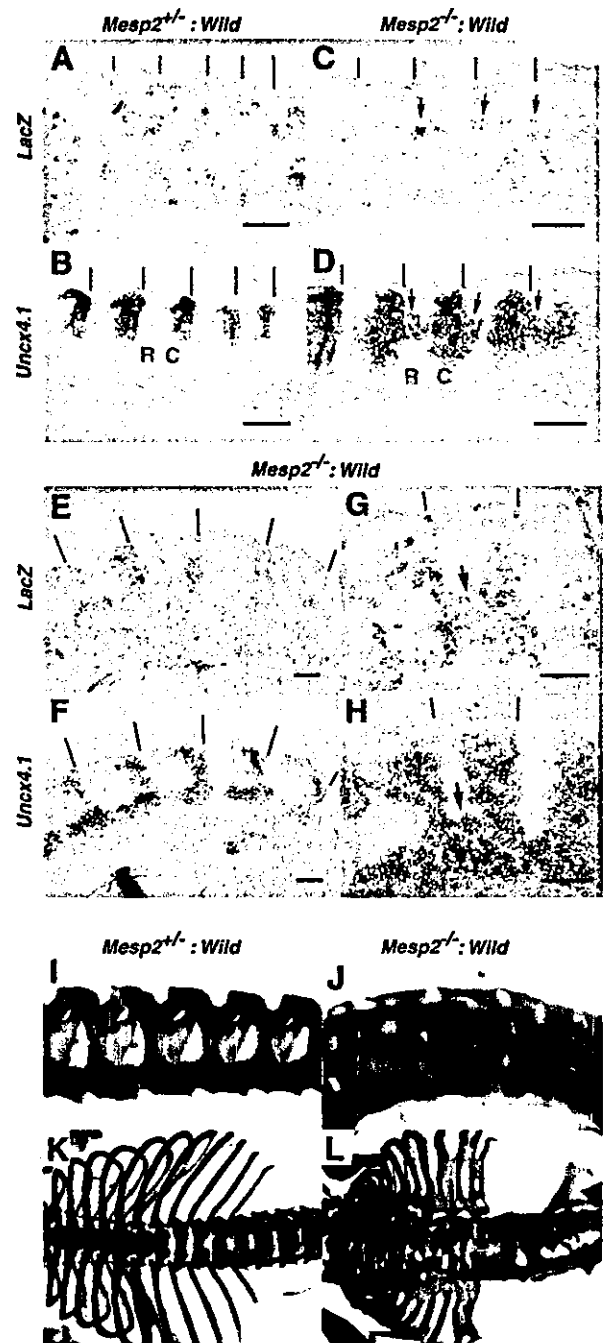

Fig. 4. Mesp2 function is cell autonomously required for rostral properties. (A-D) Expression of *lacZ* and *Uncx4.1* transcripts at the site of initial somite formation in control (A,B) and Mesp2-null (C,D) chimeric embryos. In the control, *lacZ*-expressing cells are randomly distributed and *Uncx4.1* expression is normal. In the Mesp2-null chimera, *lacZ*-expressing Mesp2-null cells at the rostral part of the incomplete segments (arrows in C) ectopically express *Uncx4.1* (arrows in D). Lines indicate somite boundaries. (E,F) In the dermomyotome, Mesp2-null cells are mostly localized at the caudal end, and the *Uncx4.1* expression pattern is normal. (G,H) In the sclerotome, the distribution of Mesp2-null cells results in expansion of *Uncx4.1* expression (arrows). (I) The control chimeric fetus shows normal vertebrae. (J) The Mesp2-null chimeric fetus exhibits partial fusion of the neural arches. (K) The control chimeric fetus shows normal ribs. (L) The Mesp2-null chimeric fetus shows proximal rib fusion. Scale bars: 100 μm. C, caudal compartment; R, rostral compartment.
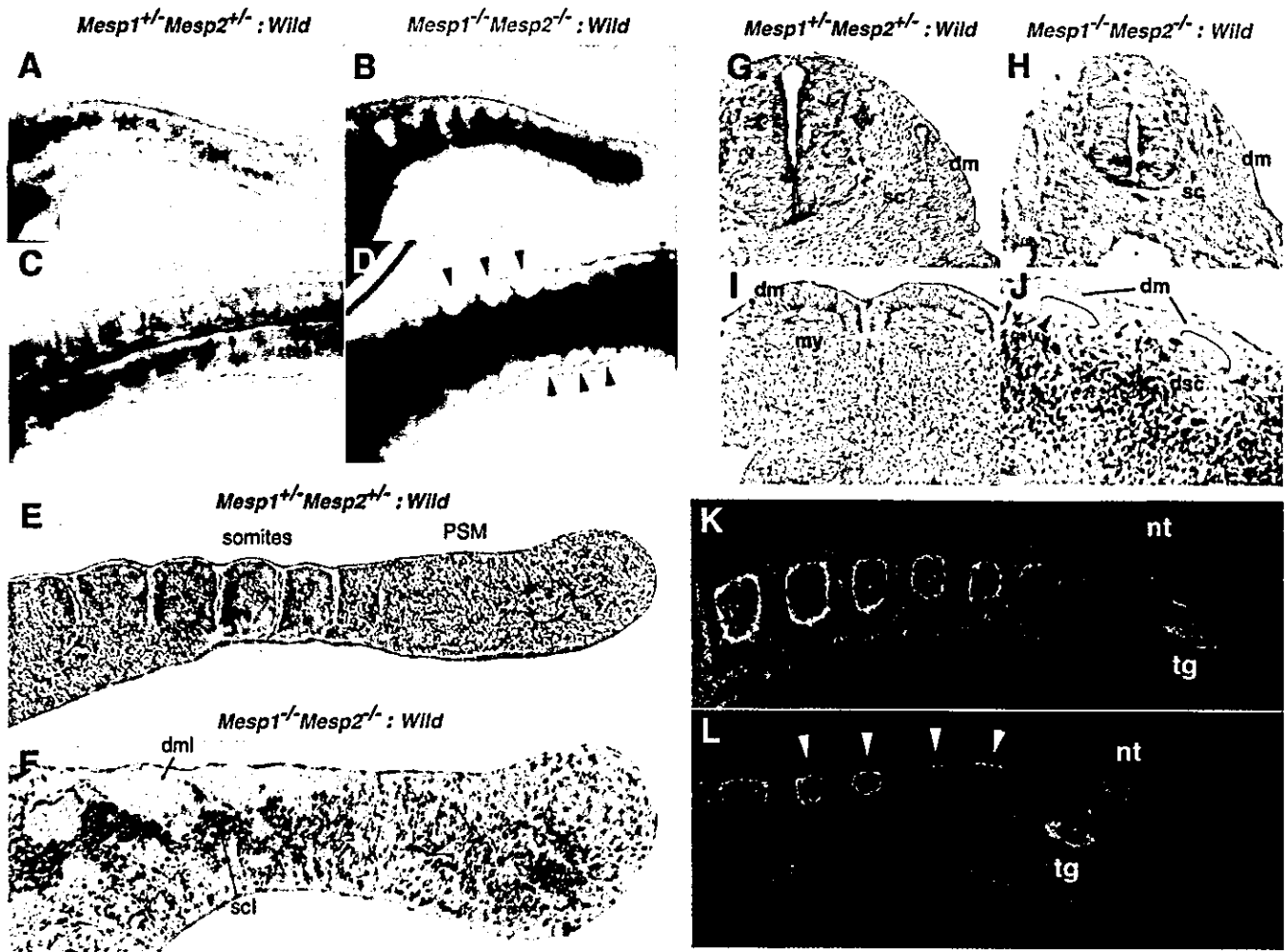
Fig. 5. Mesp1/Mesp2 double-null cells fail to contribute to epithelial somites or to the dermomyotome. (A-D) Tail regions from X-gal-stained whole-mount specimens of control (A,C) and double-null (B,D) chimeric embryos. (A,B) Lateral view. (C,D) Dorsal view. The blue double-heterozygous cells are randomly distributed in the control embryo, whereas the Mesp1/Mesp2 double-null cells are excluded from the lateral region of the somites (arrowheads in D). (E,F) Parasagittal sections of tails from chimeric embryos. (E) The labeled cells are randomly located in the control chimera. (F) The two types of cells are randomly mixed in the PSM, whereas the dermomyotome-like epithelium consisted exclusively of wild-type cells and the sclerotome-like compartment contained mostly Mesp1/Mesp2 double-null cells. Note that normal epithelial somites are not formed in this chimera. (G,H) Transverse sections show elimination of Mesp1/Mesp2 double-null cells from the dermomyotome. (I,J) The dermomyotome-like epithelium in the Mesp1/Mesp2 double-null chimeric embryo gives rise to dermomyotome, myotome (arrowhead in J) and the dorsal part of the sclerotome. Red arches indicate the inner surface of dermomyotome. (K,L) AlexaFluor 488-labeled phalloidin staining shows normal epithelialization of somites in the control chimera (K) and restriction of epithelialization in the dermomyotome-like compartment in the Mesp1/Mesp2 double-null chimera (L). dm, dermomyotome; dml, dermomyotome-like epithelium; dsc, dorsal part of the sclerotome; my, myotome; nt, neural tube; sc, sclerotome; scl, sclerotome-like compartment; tg, tail gut.

the anterior PSM. This is because 50% of cells cannot undergo suppression of Dll1 even in the future rostral half region. Therefore, our finding of a normal rostro-caudal pattern in the dermomyotome of double-null chimeras is surprising and raises the question of whether wild-type cells can be normally patterned in the presence of surrounding Mesp1/Mesp2 double-null cells. To determine how the rostro-caudal pattern in the dermomyotome is formed in the PSM, we examined the expression pattern of Dll1 (Bettenhausen et al., 1995), the stripe expression profile of which is established in the anteriormost PSM via the function of Mesp2 (Takahashi et al., 2000). The lacZ-expressing Mesp1/Mesp2 double-null cells were subsequently found to be consistently localized in the

sclerotome-like region, where Dll1 expression was abnormally expanded (Fig. 6C,D). In the dermomyotome-like region, however, Dll1 expression in the caudal half was normal. Intriguingly, strong Dll1 expression in the anteriormost PSM was suppressed in a rostrally adjoining cell population, which is mainly occupied by wild-type cells (Fig. 6C,D, arrows). This implies that wild-type cells and Mesp1/Mesp2 double-null cells rapidly segregate at S–1 to S0, after which the rostro-caudal pattern of Dll1 expression is formed in the partially segregated wild-type cell population but not in the randomly mixed cell population. In other words, the separation from Mesp1/Mesp2 double-null cells enabled normal rostro-caudal patterning of wild-type cells.
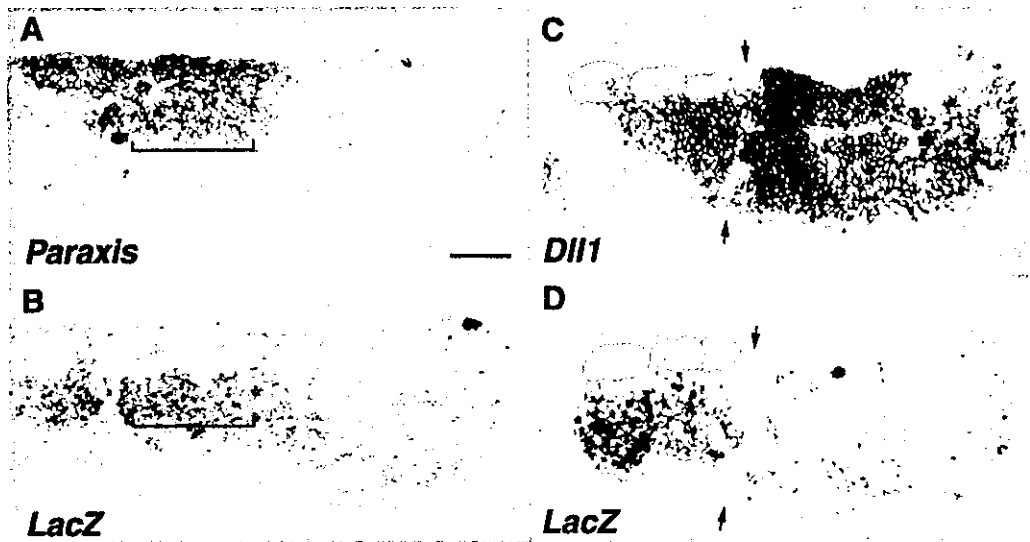
Fig. 6. (A,B) Mesp1/Mesp2 double-null cells express *Paraxis*. Adjacent parasagittal sections of the Mesp1/Mesp2 double-null chimeric embryo were stained for either *Paraxis* (A) or *lacZ* (B). Note that the expression domains of the two genes overlap in the medial sclerotomal region (brackets). (C,D) The rostro-caudal pattern in the dermomyotome is formed in a partially segregating wild-type cell population. Adjacent sections of the Mesp1/Mesp2 double-null chimeric embryos were stained for *Dll1* (C) or *lacZ* (D) mRNA. Red outlines demarcate the dorsal dermomyotome-like compartments. Note that suppression of *Dll1* expression occurs in a region mostly occupied by wild-type cells (arrows). Scale bar: 100 μm.

Fig. 7. Rostro-caudal patterning of the sclerotome is disrupted in Mesp1/Mesp2 double-null chimeric embryos. (A) The control chimeric embryos exhibit normal stripe patterns of *Uncx4.1* expression throughout the somite region. (B) The Mesp1/Mesp2 double-null chimeric embryos exhibit continuous *Uncx4.1* expression in the ventral sclerotomal region. Note that caudal localization of *Uncx4.1* expression is normal in the dermomyotome and dorsal sclerotome. The insets show a higher magnification of lumbar somites. (C,D) Adjacent sections showing that *lacZ*-expressing Mesp1/Mesp2 double-null cells express *Uncx4.1*. (E-H) The Mesp1/Mesp2 double-null chimeric fetus exhibits caudalization of the vertebrae and of the proximal ribs. (E) The control chimeric fetus

shows normal metameric arrangement of the neural arches. (F) The Mesp1/Mesp2 double-null chimeric fetus shows severe fusion of the pedicles and the laminae of neural arches. (G) The control chimeric fetus has normal arrangement of ribs. (H) The double-null chimeric fetus shows severe fusion of the proximal elements of the ribs. Scale bars: 100 μm.
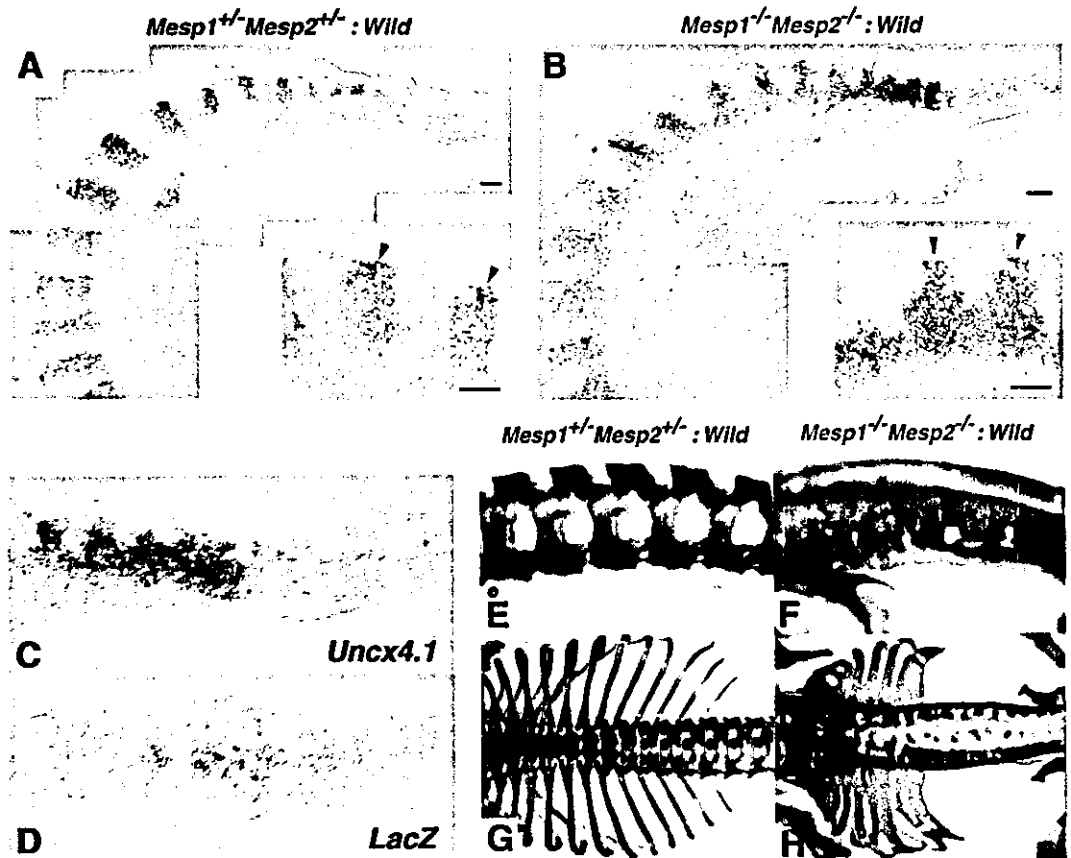
Mesp2-null fetuses display caudalized vertebrae with extensive fusion of the pedicles of neural arches and proximal elements of the ribs (Saga et al., 1997). The Mesp1/Mesp2 double-null chimeric fetuses also exhibited fusion of the pedicles of neural arches and the proximal ribs (Fig. 7E-H). Furthermore, the vertebrae of severe chimeric fetuses were indistinguishable from those of Mesp2-null fetuses. These observations indicate that Mesp1/Mesp2 double-null cells can differentiate into caudal sclerotome and possibly contribute to chondrogenesis.

Discussion

Mesp1 and Mesp2 not only exhibit similar expression patterns but also share common bHLH domains as transcription factors. Previous studies using gene replacement experiments (Saga, 1998) (Y.S. and S.K., unpublished) indicate that these genes can compensate for each other. However, the early lethality of double knockout mice hampered any further detailed analysis of somitogenesis. An obvious strategy to further elucidate the functions of Mesp1 and Mesp2 was, therefore, the generation of a conditional knockout allele for Mesp2 in Mesp1 disrupted cells in which the Cre gene is specifically activated in the paraxial mesoderm, which is now underway. Chimera analysis is also a powerful method as an alternative strategy. Comparisons of chimeras, composed of either Mesp2-null or Mesp1/Mesp2 double-null cells, made it possible to determine the contribution of Mesp1 to somitogenesis. Our results indicate that Mesp1 has redundant functions in the epithelialization of somitic mesoderm and additionally, by chimeric analysis, we were able to demonstrate the cell autonomy of Mesp1 and Mesp2 function during some critical steps of somitogenesis.

The relative contributions of Mesp1 and Mesp2 to somitogenesis

In Mesp1-null mice, epithelial somites with normal rostro-caudal polarity are generated, whereas Mesp2-null mice exhibit defects in both the generation of epithelial somites and the establishment of rostro-caudal polarity. Thus, it seems likely that Mesp2 function is both necessary and sufficient for somitogenesis. However, dermomyotome formation was observed, without normal segmentation, even in Mesp2-null mice. In view of the apparent redundant functions of Mesp1 and Mesp2 in somitogenesis, as demonstrated by our previous gene replacement study, it was possible that the Mesp1/Mesp2 double-null embryo would exhibit a much more severe phenotype in relation to somitogenesis. In our chimera analyses, both Mesp2-null and Mesp1/Mesp2 double-null cells exhibited complete caudalization of somitic mesoderm, indicating that Mesp1 function is not sufficient to rescue Mesp2 deficiency and restore rostro-caudal polarity. Likewise, both Mesp2-null and Mesp1/Mesp2 double-null cells were incapable of forming an initial segment boundary, showing that the contribution of Mesp1 is also minor during this process. By contrast, whereas Mesp1/Mesp2 double-null cells lacked any ability to epithelialize, Mesp2-null cells were occasionally integrated into epithelial somites and dermomyotome, indicating that the contribution of Mesp1 to epithelialization is significant and that Mesp1 can function in the absence of Mesp2 (Fig. 8). We therefore postulate that the epithelialization
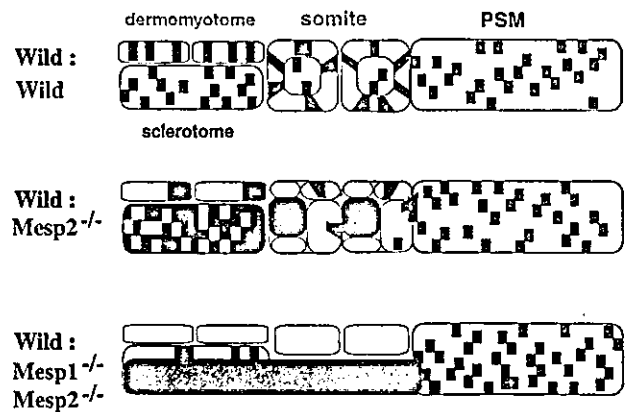

Fig. 8. A schematic summarization of the Mesp1/Mesp2 chimera experiments. Mesp1/Mesp2 double-null cells can contribute to neither epithelial somite nor dermomyotome formation, whereas Mesp2-null cells can partially contribute to both somites and dermomyotome. Red outlines indicate epithelialized tissues (epithelial somites, dermomyotomes and abnormal small clusters).

of dermomyotome, observed in Mesp2-null embryos, is dependent on Mesp1.

Mesp factors are cell autonomously required for epithelialization of somitic mesoderm but may also be non-cell autonomously required for morphological boundary formation

Conventional interpretations of the results of chimera analysis are generally based upon the regulative development of the vertebrate embryo and argue cell autonomy of specific gene functions in embryogenesis (Ciruna et al., 1997; Brown et al., 1999; Kitajima et al., 2000; Koizumi et al., 2001). Mesp1/Mesp2 double-null cells failed to form epithelial somites, even in the presence of surrounding wild-type cells. In addition, they were incapable of contributing to dermomyotome, where cell sorting occurs. This strongly suggests that Mesp factors are cell autonomously required for the epithelialization of somitic mesoderm. However, we also found striking non-cell autonomous effects of Mesp mutant cells on wild-type cell behaviors. That is, both types of Mesp mutant cell not only failed to undergo normal somitogenesis, but also inhibited the normal morphogenesis of wild-type cells. This implies that there are non-cell autonomous roles for Mesp factors in the establishment of the future somite boundary, as we will discuss further.

Initial epithelial somite formation is achieved by the mesenchymal-epithelial transition of cells located in the anterior PSM. A future somite boundary is established at a specific position in the PSM, followed by gap formation between the mesenchymal cell populations. Subsequently, cells located anterior to the boundary are epithelialized. This process is known to be mediated by an inductive signal from cells posterior to the boundary (Sato et al., 2002). Therefore, defects in epithelial somite formation can be explained in two principal ways: a lack of cellular ability to epithelialize (cell autonomous) and a lack of an inducing signal, which is produced in the anterior PSM by a mechanism mediated by Notch signaling (thus non-cell autonomous). In the case of chimeras of Mesp1/Mesp2 double-null cells, no local

boundary formed by locally distributed wild-type cells was observed, i.e. even a gap between wild-type cells was never observed in the mixture of Mesp1/Mesp2 double-null cells and wild-type cells. It is likely, therefore, that the wild-type cell population can form a boundary only after separation from Mesp1/Mesp2 double-null cells (Fig. 8). By contrast, some local boundaries between epithelial wild-type cell clusters were occasionally observed in chimeras with Mesp2-null cells. Considering that there is functional redundancy between these transcription factors, it is possible that either Mesp1 or Mesp2 is necessary for the formation of a signaling center or source of the putative inductive signal. Hence, we cannot exclude the possibility that the lack of Mesp function may affect non-cell autonomous generation of the inductive signal in the anterior PSM.

Formation of epithelial somites requires paraxis, which is a transcription factor (Burgess et al., 1996; Nakaya et al., 2004). We observed that Mesp1/Mesp2 double-null cells at the medial sclerotomal region expressed *Paraxis*, indicating that Mesp factors are not absolutely required for *Paraxis* expression. Defects in epithelial somite formation in paraxis-null embryos, with normal *Mesp2* expression (Johnson et al., 2001), and in Mesp2-null embryos, with normal *Paraxis* expression, imply that epithelial somite formation independently requires both gene functions.

Mesp2 is cell autonomously required for the acquisition of rostral properties

The distribution of Mesp2-null cells in the Mesp2-null chimeric embryos may appear somewhat paradoxical, as they are localized at the rostral side in the incomplete somites but at the caudal side in the dermomyotome. Initial localization at the rostral and central region, however, is likely to be due to the relative lack of epithelialization functions. In mammalian and avian embryos, mesenchymal-to-epithelial conversion of the PSM commences from the rostral side of the future somite boundary, i.e. the caudal margin of the presumptive somite (Duband et al., 1987). Epithelialization then proceeds anteriorly in the dorsal and ventral faces and in such a process, Mesp2-null cells, which are less able to participate in epithelialization, may therefore be pushed to the central and rostral sides. Thus, the majority of the Mesp2-null cells localize to the central, prospective sclerotomal region and a small number of them are integrated in the future dermomyotomal region. The incomplete somites then undergo reorganization into dermomyotome and sclerotome, and small numbers of Mesp2-null cells in the dermomyotome may be sorted out to the caudal end. Therefore, the apparently complex distribution pattern of Mesp2-null cells is likely to reflect a combination of defects in epithelialization and rostro-caudal patterning. In the incomplete segments of Mesp2-null chimeric embryos, the Mesp2-null cells fail to acquire rostral properties even when localized at the rostral side. Moreover, in the dermomyotome, where rostro-caudal patterning is rescued, Mesp2-null cells are mostly localized in the caudal region. These observations suggested that the requirement of Mesp2 for the acquisition of rostral properties is cell autonomous. Similarly, it has been reported that presenilin 1 (Psen1) is required for acquisition of caudal half properties (Takahashi et al., 2000; Koizumi et al., 2001) and that Psen1-null cells cannot contribute to the caudal half of somites in chimeric embryos,

showing cell autonomous roles for Psen1 (Koizumi et al., 2001).

Mesp mutant cells affect the rostro-caudal patterning of somites due to the lack of cellular interaction with wild-type cells

In a previous study, we have shown that the rostro-caudal patterning of somites is generated by complex cellular interactions involved in positive and negative feedback pathways of Dll1-Notch and Dll3-Notch signaling, and regulation by Mesp2 in the PSM (Takahashi et al., 2003). In chimeras with either Mesp2-null or Mesp1/Mesp2 double-null cells, the mutant cells were distributed evenly and did not show any sorting bias in a rostro-caudal direction in the PSM. Since both Mesp2-null and Mesp1/Mesp2 double-null cells have the ability to form caudal cells, it is likely that if wild-type cells could occupy the rostral part of future somite regions and have the ability to sort in the PSM, a normal rostro-caudal patterning would be generated. We did not observe this, however, and conclude that the presence of mutant cells lacking Mesp factors must have disrupted normal cellular interactions via Notch signaling. Thus these non-cell-autonomous effects of our mutant cells are strongly supportive of our previous contention that rostro-caudal pattering is generated by cellular interactions via Notch signaling.

References

Bettenhausen, B., Hrabe de Angelis, M., Simon, D., Guénet, J.-L. and Gossler, A. (1995). Transient and restricted expression during mouse embryogenesis of Dll1, a murine gene closely related to *Drosophila* Delta. *Development* 121, 2407-2418.

Borycki, A. G. and Emerson, C. P., Jr (2000). Multiple tissue interactions and signal transduction pathways control somite myogenesis. *Curr. Top. Dev. Biol.* 48, 165-224.

Brown, D., Wagner, D., Li, X., Richardson, D. A. and Olson, E. N. (1999). Dual role of the basic helix-loop-helix transcription factor scleraxis in mesoderm formation and chondrogenesis during mouse embryogenesis. *Development* 126, 4317-4329.

Burgess, R., Cserjesi, P., Ligon, K. L. and Olson, E. N. (1995). Paraxis: a basic helix-loop-helix protein expressed in paraxial mesoderm and developing somites. *Dev. Biol.* 168, 296-306.

Burgess, R., Rawls, A., Brown, D., Bradley, A. and Olson, E. N. (1996). Requirement of the *paraxis* gene for somite formation and musculoskeletal patterning. *Nature* 384, 570-573.

Ciruna, B. G., Schwartz, L., Harpal, K., Yamaguchi, T. P. and Rossant, J. (1997). Chimeric analysis of *fibroblast growth factor receptor-1 (Fgfr1)* function: a role for FGFR1 in morphogenetic movement through the primitive streak. *Development* 124, 2829-2841.

Duband, J. L., Dufour, S., Hatta, K., Takeichi, M., Edelman, G. M. and Thiery, J. P. (1987). Adhesion molecules during somitogenesis in the avian embryo. *J. Cell Biol.* 104, 1361-1374.

Fan, C. M. and Tessier Lavigne, M. (1994). Patterning of mammalian somites by surface ectoderm and notochord: Evidence for sclerotome induction by a hedgehog homolog. *Cell* 79, 1175-1186.

Gossler, A. and Hrabe de Angelis, M. (1997). Somitogenesis. *Curr. Top. Dev. Biol.* 38, 225-287.

Johnson, J., Rhee, J., Parsons, S. M., Brown, D., Olson, E. N. and Rawls, A. (2001). The anterior/posterior polarity of somites is disrupted in Paraxis-deficient mice. *Dev. Biol.* 229, 176-187.

Kitajima, S., Takagi, A., Inoue, T. and Saga, Y. (2000). MesP1 and MesP2

are essential for the development of cardiac mesoderm. *Development* **127**, 3215-3226.

Koizumi, K., Nakajima, M., Yuasa, S., Saga, Y., Sakai, T., Kuriyama, T., Shirasawa, T. and Koseki, H. (2001). The role of presenilin 1 during somite segmentation. *Development* **128**, 1391-1402.

Mansouri, A., Yokota, Y., Wehr, R., Copeland, N. G., Jenkins, N. A. and Gruss, P. (1997). Paired-related murine homeobox gene expressed in the developing sclerotome, kidney, and nervous system. *Dev. Dyn.* **210**, 53-65.

Nakaya, Y., Kuroda, S., Katagiri, Y. T., Kaibuchi, K. and Takahashi, Y. (2004). Mesenchymal-epithelial transition during somitic segmentation is regulated by differential roles of Cdc42 and Rac1. *Dev. Cell* **7**, 425-438.

Neidhardt, L. M., Kispert, A. and Herrmann, B. G. (1997). A mouse gene of the paired-related homeobox class expressed in the caudal somite compartment and in the developing vertebral column, kidney and nervous system. *Dev. Genes Evol.* **207**, 330-339.

Nieto, M. A., Gilardi-Hebenstreit, P., Charnay, P. and Wilkinson, D. G. (1992). A receptor protein tyrosine kinase implicated in the segmental patterning of the hindbrain and mesoderm. *Development* **116**, 1137-1150.

Nomura-Kitabayashi, A., Takahashi, Y., Kitajima, S., Inoue, T., Takeda, H. and Saga, Y. (2002). Hypomorphic *Mesp* allele distinguishes establishment of rostro-caudal polarity and segment border formation in somitogenesis. *Development* **129**, 2473-2481.

Pourquié, O. (2001). Vertebrate somitogenesis. *Annu. Rev. Cell. Dev. Biol.* **17**, 311-350.

Saga, Y. (1998). Genetic rescue of segmentation defect in MesP2-deficient mice by MesP1 gene replacement. *Mech. Dev.* **75**, 53-66.

Saga, Y. and Takeda, H. (2001). The making of the somite: molecular events in vertebrate segmentation. *Nat. Rev. Genet.* **2**, 835-845.

Saga, Y., Hata, N., Kobayashi, S., Magnuson, T., Seldin, M. and Taketo, M. M. (1996). MesP1: A novel basic helix-loop-helix protein expressed in the nascent mesodermal cells during mouse gastrulation. *Development* **122**, 2769-2778.

Saga, Y., Hata, N., Koseki, H. and Taketo, M. M. (1997). *Mesp2*: a novel mouse gene expressed in the presegmented mesoderm and essential for segmentation initiation. *Genes Dev.* **11**, 1827-1839.

Saga, Y., Miyagawa-Tomita, S., Takagi, A., Kitajima S., Miyazaki, J. and Inoue, T (1999). MesP1 is expressed in the heart precursor cells and required for the formation of a single heart tube. *Development* **126**, 3437-3447.

Sato, Y., Yasuda, K. and Takahashi, Y. (2002). Morphological boundary forms by a novel inductive event mediated by Lunatic fringe and Notch during somitic segmentation. *Development* **129**, 3633-3644.

Takahashi, Y., Koizumi, K., Takagi, A., Kitajima, S., Inoue, T., Koseki, H. and Saga, Y. (2000). Mesp2 initiates somite segmentation through the Notch signalling pathway. *Nat. Genet.* **25**, 390-396.

Takahashi, Y., Inoue, T., Gossler, A. and Saga, Y. (2003). Feedback loops comprising Dll1, Dll3 and Mesp2, and differential involvement of Psen1 are essential for rostrocaudal patterning of somites. *Development* **130**, 4259-4268.

Zambrowicz, B. P., Imamoto, A., Fiering, S., Herzenberg, L. A., Kerr, W. G. and Soriano, P. (1997). Disruption of overlapping transcripts in the ROSA beta geo 26 gene trap strain leads to widespread expression of beta-galactosidase in mouse embryos and hematopoietic cells. *Proc. Natl. Acad. Sci. USA* **94**, 3789-3794.

4．トキシコゲノミクス

菅野 純　相﨑健一　五十嵐 勝秀　小野 敦　中津則之

遺伝子発現カスケード解析を目指した形質非依存型トキシコゲノミクスに適用するため，マイクロアレイから細胞1個当たりのmRNA絶対量を得る方法（"Percellome"）を開発した．これにより遺伝子発現量を，ゼロを起点とする均等目盛りで表示し直接比較することができるようになった．対照群も処置群も無理なく同列に表示することができ，さらなる標準化操作が原則的に不必要となったため，測定し得たすべての遺伝子についてマイクロアレイ間はもとより，実験間での直接比較が行えるようになった．この特長は，生物学者が内容を直感的に把握しやすいようなデータの可視化にも役立ち，その後のデータ解析とインフォマティクス形成を促進することが示されつつある．本システムは大型プロジェクトを対象として開発したものであるが，実際には小規模の実験サンプルに対しても有用性が高いことが実証されている．特に変動遺伝子リストの遺伝子数が飛躍的に増大することが多い．それは，変動比率による足切りやハズレ値計算のような統計手法を用いる必要がなく，個々の遺伝子について逐一比較検討ができるためである．異なったプラットフォーム間でのデータ互換にも拡張可能であり，研究規模やプラットフォームの種類にかかわらずデータをもちより，相互にデータを直接比較することが可能なコンソーシアムを構築することに本手法が貢献することが期待される．

ゲノム創薬と薬理ゲノミクス

はじめに

　毒性学は，生物界（biosphere）と化学物質界（chemosphere）との相互作用を解析し，現実に起きてしまった有害作用（薬の副作用，健康被害など）の把握，評価，対策のみならず，そのような事態の未然防止を目指す学問体系である．例えば，PCB（ポリ塩化ビフェニール）はその電気抵抗性，熱安定性，低反応性などから，工業的に優秀な材料として熱交換や絶縁に汎用された．この物質の毒性知識が早期に浸透していれば食品を直接加熱する熱媒体にPCBを用いる

という発想は回避されたのかもしれない．当時の生物学・臨床医学・病理学・毒性学では，PCBのような化学物質の生体影響は，肝臓などでの代謝酵素（P450など）の誘導現象として把握されていたが，その基礎となるリガンド依存的転写因子群（AhR，CAR，PXRをはじめとするorphan受容体群）とその関連シグナル伝達に関する事象が明らかとなってきたのは比較的最近のことである[1]．その結果を受けて胎児影響を含む毒性の分子機構が明らかになるに連れて，実際にどの程度の暴露が，どの発達時期の人体に，どのように有害であるかの判断がより正確にくだせるようになり

Jun Kanno / Ken-ichi Aisaki / Katsuhide Igarashi / Atsushi Ono / Noriyuki Nakatsu : Division of Cellular & Molecular Toxicology, Biological Safety Research Center, National Institute of Health Sciences（国立医薬品食品衛生研究所安全性生物試験研究センター毒性部）

つつある．さらには，個人を対象とした毒性評価から，集団（日本国民全体）を対象としたそれまでを，広く見渡すことが要求される．例として有名なのは，PCB暴露によるIQ低下論議である．ある集団のIQが5ポイント下がると，何らかの介護を必要とする人々の数が著増するというものである．すなわち，平均的なIQをもつ個人のIQが5ポイント下がっても実質上問題はないが，社会集団としての影響は無視できないという問題である[2][3]．科学的には，高感受性亜集団，個体差，動物実験データからヒトへの外挿に際しての種差問題などが関連する．

近年の健康ブームは，いわゆる「サプリメント」など，健康に有益な効能を示唆あるいは謳う一連の食品関連製品を生み出している．他方の医薬品については「薬効」と引き換えに「副作用」が常に考慮されることから，使用者のcost-benefit（費用便益・費用対効果）の概念を基礎に，取り扱いの体系ができあがっており「処方箋」が必要であったり，注意書きが添付されていたりする．これに対してサプリメントなどは食品，および食品に由来する成分からなるとされることから，「食経験」にもとづいた安全性の概念が基本となっている．しかし，食品も医薬品も，生活の利便性のために毎日利用する化学物質も，体内で生体分子と相互作用を起こす．それらの毒性評価を生体側からみると，身体に入るまでの「物質の分類」や「能書き」はもはや重要ではなく，身体に入ったあとにどのような反応が如何に惹起されるかが問題となる．

人体に化学物質が何を引き起こすかを検討するためには，ヒトからの情報を得ることが一番正確なことはいうまでもない．薬の開発の過程では，ヒトによる「臨床試験」が可能である．この場合の毒性には，用量作用関係の概念が乏しい．すなわち，実際に薬として投与するときの薬用量において，どのような毒性（副作用）があらわれるかが，最大の焦点であり，わざわざ「自殺目的」の大量投与を行うことはなく，薬効が期待できない微量投与も行わないわけである．これに対して，いわゆる化学物質，例えば，家庭用品，工業製品，食品添加物などの現代生活の利便性に欠かせない物質に由来する化学成分の体内への侵入に対しては，一般的にcost-benefitの概念が弱く働き，可能ならばゼロにしたいという傾向がある．しかし，「完全ゼロ」は使用する限り基本的には不可能であるの

で，どの位の量までなら安全と見なせるかを検討することが行われてきている．これらについては，人体実験が倫理的にも現実的にもできないと考えるのが通常である．なお，薬でも「人体実験」が事実上できない対象がある．それは，胎児と子供である．いずれの場合も，現在のところ，人の身代わりとしてモデル動物を用いることになる．他方，食品そのもの，あるいは食品の主成分については「食経験有り」＝「安全」という考えの下に，毒性評価を行ってきていないのが現状である．しかし，成分などの濃縮や抽出により錠剤やエキスの形を取るサプリメントでは少なくとも「調理法」と「摂取量」のコントロールが「今までの経験の適用外」となる場合が多い．このようなものが「処方箋なし」に利用される場合の安全性を検討する際に，人体実験を行うか，動物実験を行うか，動物で得た情報はどのようにヒトに適用するのか，などが問題となる．

化学物質の毒性の量と質の問題

多量に摂取すれば毒性は強く，少量になれば毒性は弱まるという大原則（毒性は用量に関して単調増加する）の下では，「毒性に閾値がある」と考えられる場合と，「閾値が存在しない」と考えられる場合とで扱いを分けている．前者の場合は無毒性量あるいは無作用量を実験動物で求め，種差や個体差を勘案した係数（不確実係数あるいは安全係数と呼び，通常100を用いる）で除して，安全の目安となる基準値とする．後者の場合は，無毒性量の代わりに，俗に「運悪く雷に打たれて死ぬ確率」を目安とする実質安全量（virtually safe dose，通常10^{-5}ないし10^{-6}の危険率を適用）を採用し，同様の手続きを経てヒトへの外挿を行っている．これらの判断が正しいか否かを検討する材料としては人での中毒事例，自殺事例，事故事例やそれらに関する疫学調査が活用され，それにもとづく基準設定法の修正が折にふれて加えられてきた歴史がある．ところで，食品あるいは食品関連製品（サプリメントなど）の場合，安全性評価に不確実係数100を使用するとどういうことになるであろうか．例えば，ニンニクや玉ねぎを毎日1個食べても安全であるという結果を引き出そうとすると，実験動物に毎日100個相当を食べても何も起こらないことを示す必要がある．
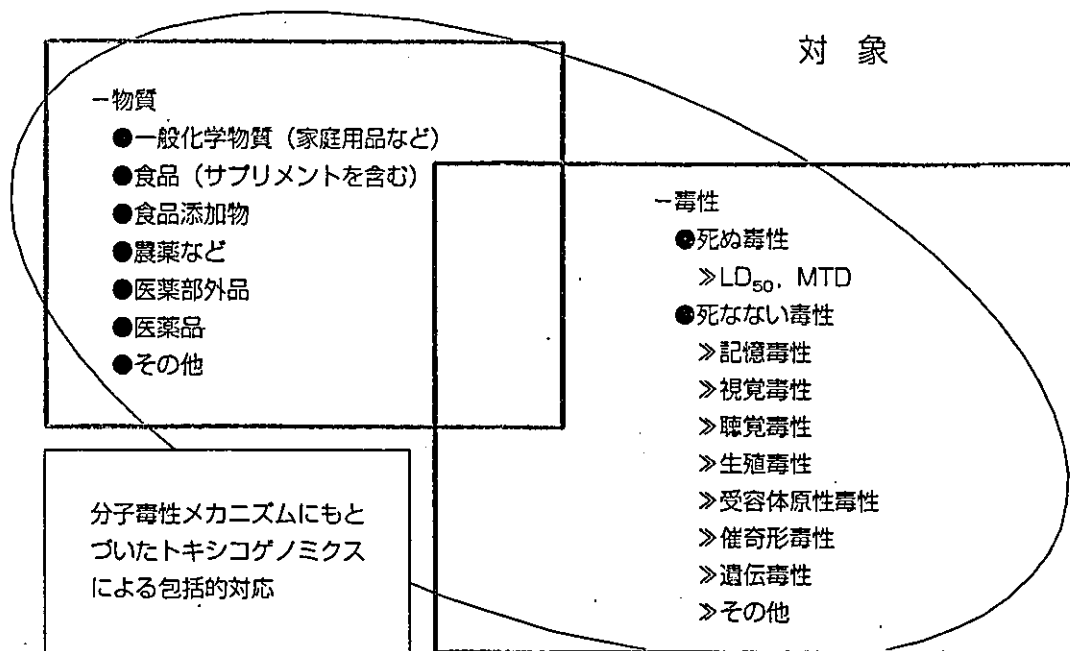
図1　分子毒性メカニズムにもとづいたトキシコゲノミクスが目指す包括的毒性
　　毒性を分類する際に，物質のカテゴリーを用いたり，毒性の症状を用いたりする．しかし，生
体側からみれば，体内に入った物質がどのような生体反応を誘導するかが問題である．分子毒
性メカニズムにもとづいたトキシコゲノミクスでは，生体反応を遺伝子発現カスケードとして
把握することにより，このような従来の分類を包括した対応を目指す

ニンニクや玉ねぎ中のアリシンが動物に溶血を引き起こすが，100倍量を摂取すれば影響がみられる可能性が高い．すなわち，食品に関して動物実験を行った場合，一般論として不確実係数は利用できず，問題とする成分に対する生体反応のヒト・動物間の種差そのものを検討することが必要となる．

　毒性の質的な問題はどのように取り扱われてきたか．生物学が現象の記述学に基礎を置いていた段階での毒性学は，対象が医薬品であれ，一般的な化学物質であれ，その要求される役割を果たすために，投与された化学物質と症状との連関性にもとづいた化学物質の体系化を基盤として発達してきた（図1）．その過程でのさまざまな経験を取り入れる形で，前述の「不確実係数」や「LD$_{50}$」の概念が利用され，現在まで，非常に有効に機能してきている．ここまでの毒性学は，化学物質の投与とそれによる症状（毒性）発現の関連性を分類し体系化するものであり，実験動物と人とをつなぐために，回帰モデル（regression model）の概念に根差した後向きの検討が行われることが多かった．しかし，サリドマイド禍（奇形発生）に象徴されるように，げっ歯類の実験動物では毒性が確認されず，人に使用して初めて催奇形性が明らかになった事例の存在は，この方法の限界を示している．

火事場の現場検証？

　近年，科学の進歩により，毒性学は生体内で引き起こされる反応の分子レベルから形態レベルまでのメカニズム記述を基礎とするものへと変貌しつつある．ここで，活躍するのがハイスループット性の高いマイクロアレイ技術である．しかし，マイクロアレイから得られた遺伝子発現プロファイルによる検討も，そのときに観測される毒性形質と関連付け，いわゆる化学物質のフィンガープリント（指紋）として毒性反応の類型化を行うことが多い．このような関連付けを「phenotypic anchoring」と呼ぶことがある[4]．

　分子毒性学の立場からは，化学物質が生体内で引き起こしている一連の事象を理解することが直近の目標である（図2）．毒性所見が明瞭に現れた段階では，化学物質による遺伝子発現はすでに十分にタンパク発現を引き起こしており，その結果としての組織改変までも完了してしまっている．この段階での遺伝子発現プロファイルは，所見と直結したものであることに間違いはないが，そこに至る過程を端的に示すものでは
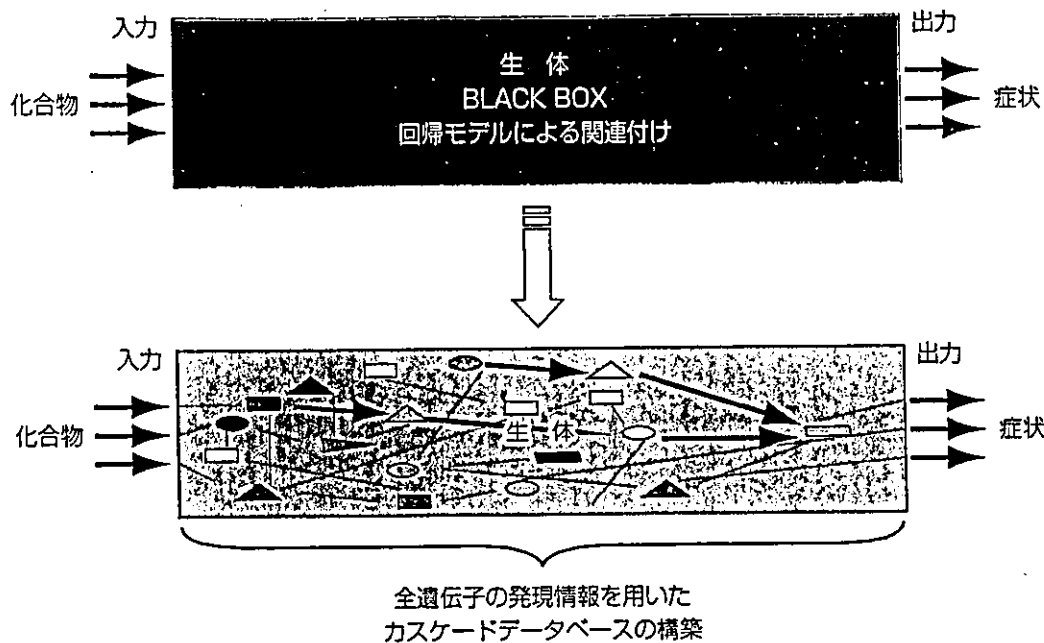
図2 経験則からメカニズムによる予測へ
生物学が現象の記述学に基礎を置いていた段階での毒性学は、投与された化学物質と症状
との間を回帰モデルにより関連付けることで体系化が行われてきた。しかし、分子毒性学
の立場から一番知りたいことは、生体内で実際に起こっている一連の事象であり、遺伝子
発現解析の場合にはすべての遺伝子の情報をもとにした遺伝子カスケードの全容解明であ
る。毒性学的に重要なマーカー遺伝子（数十～数百のことが多い）についてのこのような
データベースは存在するが、ここではすべての遺伝子を対象としたものを指向する

必ずしもない。丁度、火事場の現場検証で出火元を特定する作業に似ている。これに対する別のアプローチとして、出火直後の変化から逐次検索することが考えられる。すなわち、化学物質に暴露され始めた初期からの遺伝子カスケードの全容解明である（図2）。全ゲノムが明らかになった現在、形質発現の有無にかかわらずすべての遺伝子の発現をモニターするこのようなアプローチ、すなわち「形質非依存型トキシコゲノミクス（phenotype-independent toxicogenomics）」を考慮せざるを得ない。

　動物実験を主な手段として駆使しうる立場からは、この目的のための実験プロジェクトを企画することが可能である。タンパクのリン酸化や発現の変化も同時に観測できれば理想的であるが、それらに関する網羅的観測手法が整っていない現段階では、マイクロアレイ技術による遺伝子発現が頼りである。十分に精密かつ実態的に生体反応が記載されれば、従来の膨大な時間と費用のかかる長期毒性試験（ラットなどを用いる）の代替として、より早く、安く、正確な評価、さらに、種差や個人差を勘案した正確なヒト毒性予測が

可能となることが強く期待される。特に胎児、新生児、小児、成人、老人の各発達段階における生体側の反応様式・感受性の変化や、複数の物質の進入による複合作用なども包括的に扱えるようになると考えられる。マウスにおいては遺伝子ノックアウト手法により遺伝子ごとの機能解析が可能であり、ヒトではSNPs解析が同様に利用できるであろう。これらについても、形質発現が伴わないために解析が行き詰まった場合には、形質発現に依存しない手段を選ばざるを得ない。恒常性維持機構に深くかかわる内分泌かく乱化学物質の問題など、外界からの影響が効率よく中和されてしまい、形質変化がモニターしにくい対象を扱う場合にも、形質発現の有無にかかわらずmRNAやタンパクの発現修飾を観測することが有効な影響解析手段となることが考えられる。

　今後の毒性学における遺伝子発現解析（transcriptome）、すなわちトキシコゲノミクス（toxicogenomics）は、従来の「形質依存型」のものに「形質非依存型（phenotype-independent）」のものを加える時期にきているといえよう。

形質非依存型トキシコゲノミクス（phenotype-independent toxicogenomics）の条件

形質依存型では，ある特定の毒性所見に連関した遺伝子をマーカーとして選択し，それが毒性発現に重要であると認定することから始まる．これに対して，形質非依存型トキシコゲノミクスは，まずは形質発現情報などの情報を用いずに，自らの遺伝子発現プロファイル情報のみを頼りに遺伝子発現変化の解析を開始しようとする点に特徴がある．このためには，測定するすべての遺伝子はどれも平等に重要であると仮定する必要がある．そして，そのすべてがどれだけ変動したかを正確に観測する必要がある．さらに，幾多の実験の結果を統合してはじめて全体像が明らかになるため，複数の実験の結果を長期にわたり集積し，それらのデータを縦横に解析する必要がある．

この条件を満たすためには，今までのマイクロアレイ手法には問題があった．まず，マイクロアレイの性能として，mRNAの測定可能な範囲が比較的狭いためにチップ1枚当たりに用いる総mRNA量を一定量に揃える必要があった点である．この場合，サンプル中の細胞1個当たりのmRNAの絶対的な多寡に関する情報は消失してしまう．これを補う種々の標準化手法が編み出されている[5]～[12]が，それらは原則的には統計学的な有意差検定をもとにした変動遺伝子の抽出を行う．このような計算では，一般に大半の遺伝子はサンプル間で不変であるとの前提から，多数の遺伝子が「変動したとはいえない」と位置付けられることが多い．また，変動を表現するために対照サンプルに対する比率表示をすることが多い．この場合，異なる時期に実施した複数の実験から得られたデータを比較する際に，対照群の実験間変動を吟味することが難しいという問題が加わる．

細胞1個当たりのmRNA絶対量を得る方法

このような問題を解決し，形質非依存型トキシコゲノミクスに適用するため，われわれは，細胞1個当たりのmRNA絶対量を得る方法（"Percellome"）を，当時それに必要な条件を満たしていたアフィメトリク

ス社のGeneChip®を対象に開発した（特許出願中，投稿中）．このシステムは大きく4つの要素からなっている．

①RNA用に準備したサンプル破砕液の一部からそのDNA濃度を簡便に測定する方法：細胞1個当たりのmRNA情報を得るために，サンプルを構成する総細胞数を測定する．実際に細胞数を計測することは特に実質臓器の場合には困難であるため，その代替指標として細胞核内のゲノムDNA量を用いる．サンプルをDNA測定専用に消費することを避けるため，RNA調整用の組織破砕液の極一部（通常，10μl）からDNAを測定するプロトコールを確立した．

②用量関係を考慮し工夫された多段階濃度スパイクカクテル（GSC：dose-graded spike cocktail）の調整と，それの破砕液への添加法：細胞1個当たりのmRNAの標準として，組織破砕液に添加するスパイクRNAには，GeneChip®が使用者のために用意していた5種類の枯草菌由来遺伝子のRNAを用いた．5種類の枯草菌RNAをおのおの約2,000塩基の長さに合成し，5段階の用量に配合したカクテルを作製した．これにより，広い濃度範囲をカバーする標準用量作用曲線をすべてのサンプルに導入することが可能となった．

③Hill式にもとづいた絶対化アルゴリズム：GeneChip®では，蛍光シグナルとmRNA量との間にHill式に従う関係が成立することを後述のLBM標準サンプルなどにより確認した．その結果からHill式の直線化式によりGSCを直線化して絶対量化を行う変換アルゴリズムを開発し，それを自動実行するプログラムを独自に開発した．

④マイクロアレイの用量相関性確認およびバージョン間・プラットフォーム間データ変換対応のためのLBM（liver-brain mix）標準サンプルおよびデータ変換アルゴリズム：遺伝子発現プロファイルが大きく異なる一対の組織を一定の比率で相互に希釈しあったサンプルセットを表記の目的のために用意した．具体的には，肝と脳を用い，100：0，75：25，50：50，25：75，および0：100の混合比の5サンプルからな
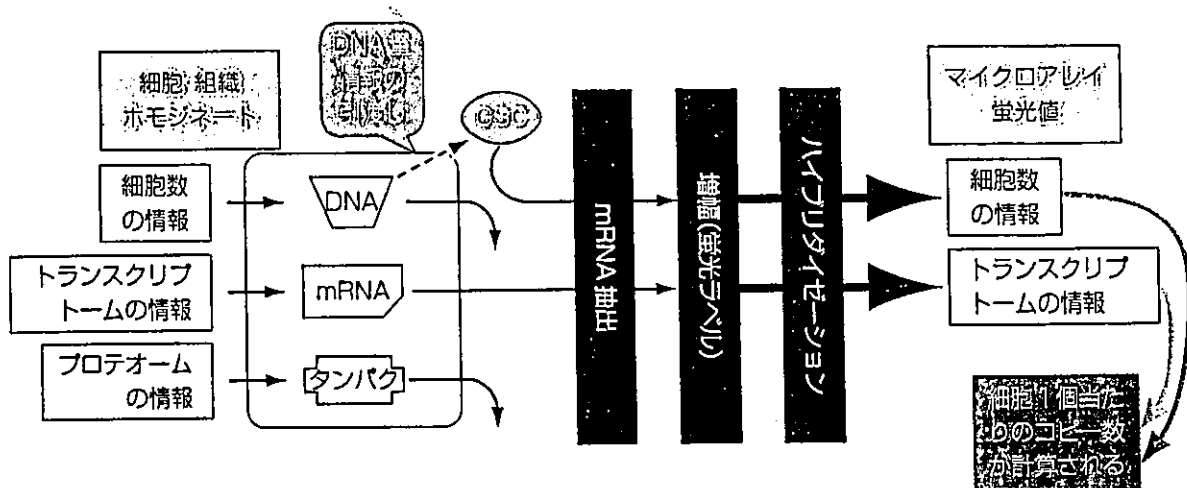
図3　絶対量化の原理
マイクロアレイなどから絶対量を得る方策は，まず，サンプル・ホモジネートのもととなった検体の細胞数の情報をDNA量として捉える．mRNA抽出段階でこのDNA情報が失われてしまうことを回避するために，DNA量の代わりに相当量の多段階濃度スパイクRNAカクテル（GSC）を添加する．mRNA抽出以降，GSCとサンプルのmRNAがともに増幅・蛍光ラベリング，マイクロアレイ表面へのハイブリダイゼーションなどの段階をほぼ平等に経験する．その結果，マイクロアレイの蛍光値を適切に比較・補正することにより，mRNAの細胞1個当たりのコピー数が計算される

るセットを用意した．

　絶対量化の基本的原理は，サンプルの細胞数（ゲノムDNA濃度で代替）に比例した分子数のスパイクRNAを添加することで，サンプルの細胞1個当たりのmRNA絶対量（コピー数）の指標をサンプル中に導入するものである（図3）．ただし，スパイクRNAは1点を規定するものではなく，5種類の枯草菌遺伝子に対するRNA（哺乳類の配列と交叉しない）を適切な公比をもたせて5段階の濃度に割り振ったカクテルとして用いることが特長である．これにより，絶対コピー数の指標になると同時に，広い用量範囲について検量線を各サンプルに導入したことになり，mRNA抽出からGeneChip®の蛍光測光までの過程で生じるデータ全体の歪みを補正する際に威力を発揮する

　他方，チップ内での異なる遺伝子の発現量の正確さに関しては，GeneChip®のプローブセットの設計に依存する．アフィメトリクス社はプローブの設計に際してそれらのTm値を一定に保つアルゴリズムを用いている．これについては，利用者として個々に定量的PCRなどにより検証する必要がある．本手法の特徴の1つとして，真の値が明らかになった時点で，すべての既測定値を一括修正することが可能であることがあげられる．

LBM（liver-brain mix）標準サンプルとの組合せ

　LBMは実験動物サンプルに対しては肝と脳の組合せを用いたが，遺伝子発現プロファイルの異なるペアであればどのような組合せでも利用可能である（ヒトサンプルに対しては2種類のヒト培養細胞株も可）．複数のペアを併用すればさらに精度のよい検定が可能となる．GSCをDNA濃度に応じて添加したLBMセットを測定し，絶対量化した結果は，グラフ化すると直線を描くはずであり，さらに50：50のサンプルで除した場合，理想的にはすべての遺伝子が50：50のところで1の値を取り，100：0あるいは0：100では0から2の間の値を取るところの直線を描くはずである．この結果から，マイクロアレイの定量性が確認される．

　さらに，LBMをバージョンアップ前後の新旧GeneChip®で測定しておくことにより（図4），LBMに含まれるすべての遺伝子（プローブセット）について，5点からなる新旧のチップ間の換算関数を求めることができる．LBMに他の臓器の組合せを用いることで取り扱える遺伝子数を増やすことが可能である．

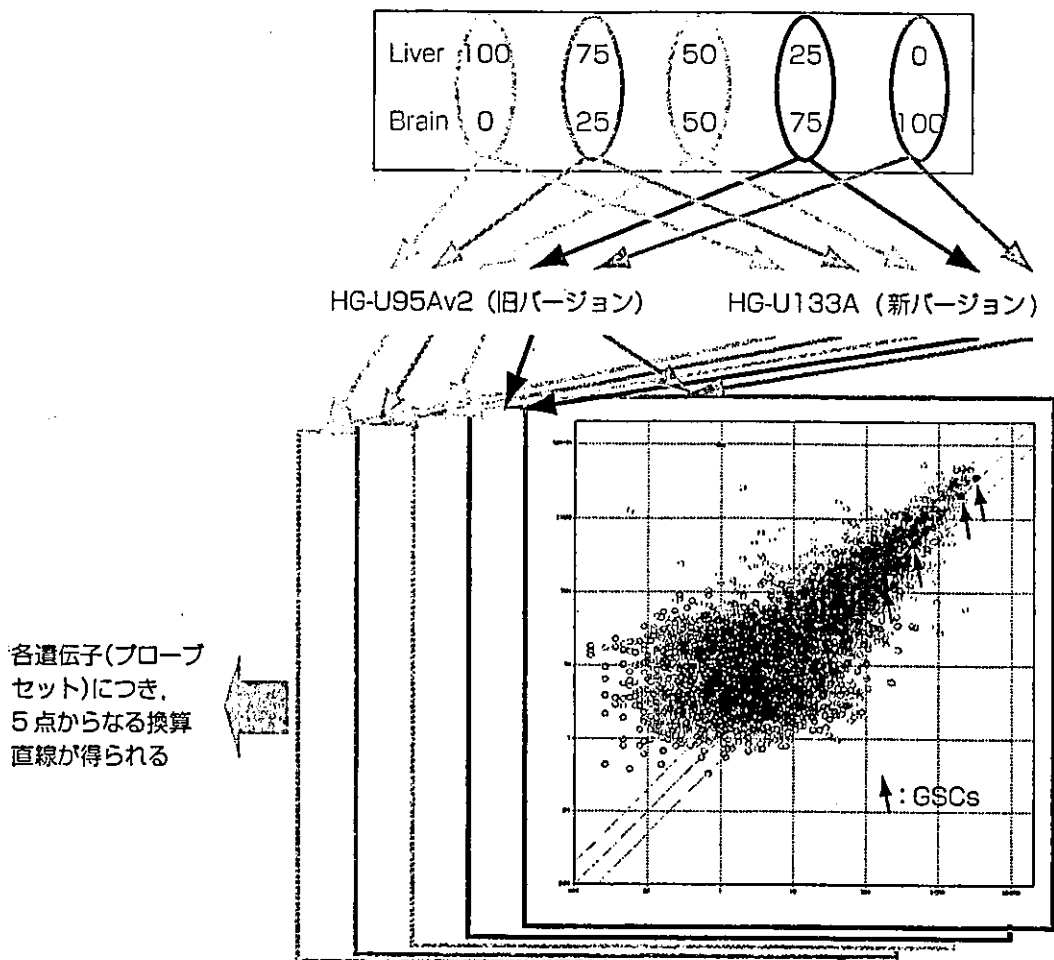　本システムのGSCを添加したサンプルはスパイクRNAを検出するプライマーセットを用意することでPCRにおいても容易に絶対量化データを得ることができる．詳細は他に譲るが，プライマーペアの増幅効率

図4　GeneChip の新旧バージョン間のデータ互換
LBM サンプルセットを新旧のバージョンの GeneChip® において測定する．スキャッターグラフで示すような関係が5組得られる．矢印で示す黒丸が GSC である．ここにプロットされた遺伝子（両バージョンに同一または対応するアノテーションが得られ，かつ，LBM サンプルに発現されているもの）については個々について直接変換式が得られる．これは，定量的PCRやアフィメトリクス社以外のマイクロアレイプラットフォームにも拡張可能である

のばらつきを勘案した絶対化アルゴリズムとともに Percellome 定量PCR システムを構築中である．GeneChip® 以外のプラットフォームとのデータ互換も可能である．本システムが適応可能なプラットフォームの条件としては，GSC を受け付けるプローブセットが用意されていること，および用量相関性が確保されてることの2点を満たしている必要がある（図5）（現在，2社の製品について検討開発中）．

遺伝子カスケード解析を目指した形質非依存型トキシコゲノミクスへの適用

厚生労働科学研究費のプロジェクトにこの Percellome システムが採用され進行中である〔厚生労働科学研究費補助金 H14-トキシコ-001（創薬支援トキシ コゲノミクス）および H15-化学-002（化学物質トキシコゲノミクス）〕．4～5段階の用量（公比√10 等）について，4時点（2，4，8，24時間等）での遺伝子発現を観測する16～20群（一群3匹）の構成からなるプロトコールにより，1つの化合物について48～60匹の動物のサンプルから Percellome データを生成している．化学物質トキシコゲノミクスプロジェクトでは，遺伝子の発現値を3次元表示することでその用量・時間依存性を視覚化し，データ解析を進めている．X軸に用量，Y軸に時間，Z軸に発現量（ゼロからの均等目盛り表示）をプロットすることにより，1つの遺伝子につき16～20格子点（48～60枚の GeneChip からのデータ）からなる1枚の局面を描くことができる（図6）．1つの GeneChip が45,000の プローブセットからなる場合，1つの化合物の用量・
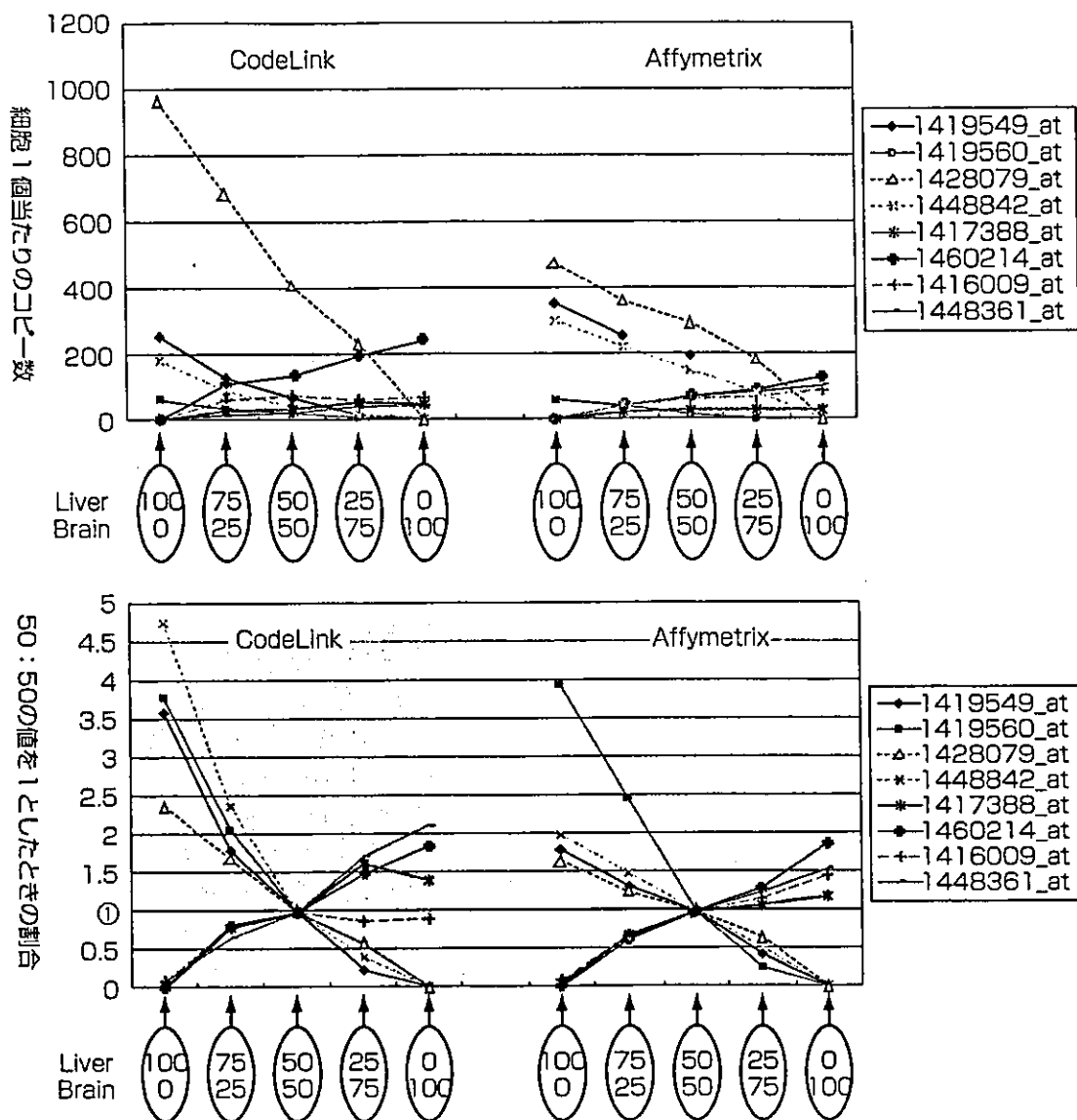
図5 LBM標準サンプルセット（Liver-Brain Mix）によるシステムの定量性の検定とデータ直接変換式の生成

LBMの5サンプルをAffymetrix社 GeneChip® (MOE430v2) および，Amersham社CodeLinkアレイ（GSCが測定可能な試作品）にて測定した．ここでは，共通に測定された8遺伝子（AffymetrixのIDにて表示）を示す．上段は，細胞1個当たりのコピー数で表示したもの．下段はLBM（50：50）の値に対する比を表示したもの（理想的には，すべての遺伝子が50：50のところで1を通り100：0におけるy切片が0〜2の範囲に収まる直線を描く）．個々のprobe setには若干の性質の相違があるが，押しなべて直線性がよく，2社間のデータの相互直接変換関数が求められる．別途に真のコピー数が判明した際（定量PCRなどにより）には，その値をもとに過去のマイクロアレイ・データを一括変換することが可能となる

時間依存的データ3次元表示では45,000枚の局面の層状集合体からなる 多層構造からなる菓子などになぞらえミルフィーユ・データ [millefeuille (MF) data] と名付けた．このMF dataは1局面の各格子点が3匹の動物に由来する3つのデータにもとづいており，格子点のデータの信頼性の評価，artifactの除去や，生物学的な蓋然性を有する変化であるか否かの判別に適しているうえに，類似の用量・時間反応を示す遺伝子の選別に威力を発揮する．

生体反応の分子メカニズム解析（カスケード解析）を目標に，遺伝子欠失動物の活用を見込んで，マウスを用いた実験を重ね，2004年6月現在で約25の既知化合物についてのデータ収集を終え，向こう2年の内に90化合物のデータを蓄積する予定である．まずはすべての遺伝子が平等に重要と考える方策を取るため，生物学者が視覚的に確認できるMF dataを利用した完全な教師なし（unsupervised）クラスタリングを開発・実施している．[NTTコムウェア株式会社